

Design and Electromagnetic Analysis of Microstructured Holey Optical Fibres with Stepwise Random-Air-Hole Distributions in Concentric Cladding Layers

Jeong I. Kim¹

¹Professor, Department of Electric, Electronic and Communication Engineering Education, Chungnam National University, Daejeon 34134, South Korea.

Abstract

As distinctive variants of the microstructured holey optical fibre (MHOF), stepwise random-air-hole optical fibres (SRHOFs) are first proposed, and design parameters are explained in order to find out influences of air-filling fraction (AF) conditions of randomized air holes in stepwise cladding regions and obtain small effective area and fairly reasonable dispersion characteristics for sensor or nonlinear device applications. Based on two computational techniques of finite-difference time-domain (FDTD) method and finite difference method (FDM), several propagation characteristics such as normalized propagation constants, chromatic dispersions, electromagnetic fields, and effective areas are investigated. This new type of design approach can be expected to be useful from the point of view of manufacturing processes and fabrications of variety fibre-optic components.

Keywords: FDTD, FDM, SRHOF, Air-filling Fraction, Chromatic Dispersions, Nonlinearity

I. INTRODUCTION

Since the invention of photonic crystal fibre (PCF), also broadly known as the microstructured holey optical fibre (MHOF) in the mid 90's, a great deal of interest in the optics and communication communities has focused on this new kind of optical fibre during the past decades [1–5]. Basically, PCFs are optical waveguides with two-dimensional periodic microstructures. If in an optical fibre uniform and identical air holes with some type of periodic arrangement run along the direction of wave propagation, such fibre is referred to as a PCF. On the other hand, some investigators have suggested that the air hole arrangement, while maintaining a regular pattern, may not be periodic or may even be completely random in shape, size, and location and yet provide light guidance [6–10]. An important feature of the PCF or random holey fibre is that it can be made of only a single material, in contrast to all other types of fibres, which are manufactured with two or more materials.

Because of its unique structure, which is different from those of the conventional step-index or graded-index fibres, the PCF or MHOF can provide propagation properties not easily attainable from conventional fibres [11–14]. For example, the MHOF can be designed to be single-mode over the entire wavelength range of interest in optical communications,

provide small and nearly constant dispersion over a wide wavelength range, or be a highly nonlinear optical fibre [9,11]. This novel fibre offers the potential for a variety of applications such as high-power lightguide with low loss, supercontinuum generation, grating-incorporated tunable filter, pressure sensor, and polarization maintaining fibre [15–18].

In this paper, stepwise random-air-hole optical fibres (SRHOFs) as distinctive variants of the PCF are first proposed, and design parameters are explained in order to investigate influences of air-filling fraction (AF) conditions of randomized air holes in stepwise cladding regions and obtain small effective area and fairly reasonable dispersion characteristics for nonlinear device applications. This new type of design approach can be expected to be useful from the point of view of manufacturing processes and fabrications of variety fibre-optic components.

II. DESIGN OF OPTICAL FIBERS WITH STEPWISE RANDOM-AIR-HOLE CLADDING REGIONS

Cladding regions of proposed holey fibres consist of random air holes stepwise-distributed in concentric hollow-cylinder-shape layers. The cylinder layers with randomly-distributed air holes along a constitutional common glass material can provide light confinement and hence guidance of the light signal. In this way, two types of holey fibres with stepwise random-air-hole distributions in concentric hollow-cylinder-shape layers outside of the core region are designed in order to compare wave-guidance properties and search for advantages among those SRHOFs.

By using air-filling fraction (AF), which is defined as the ratio of air to background glass material in each concentric hollow-cylinder-shape layer, the first type SRHOF has the AFs stepwise-decreasing as the radius from the core center increases outward in a cladding region. And the other one is retrofitted with the AFs of cylindrical layers stepwise-increasing from the core to outer cladding.

For practical consideration, these new features are constructed with only three concentric hollow-cylinder-shape layers, because it has been discovered that most light energy is largely confined to the core region and a cladding region close to the core plays an important role on guidance characteristics [5]. As shown in Fig. 1, three layers with randomized air holes are noticed, consisting of a cladding region.

Here, the core has a radius of r_1 , and the first hollow-cylinder-layer just outside of the core has the outer radius of r_2 . And the radius of the boundary between the second hollow-cylinder-shape layer and the third is equal to the distance (r_3) from the core center. Also, more shaded small holes illustrate the air regions, which could be filled with gas or liquid material for special application purposes.

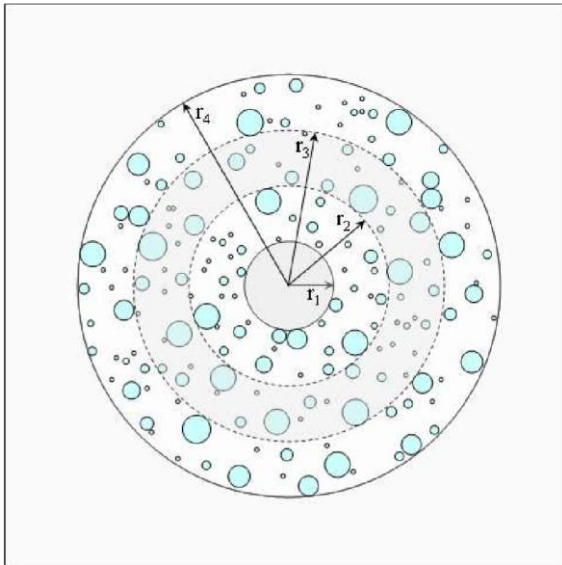


Fig. 1. Cross-sectional view for the proposed SRHOF with three concentric hollow-cylinder-shape layers in the cladding region

Based on these design methodologies to obtain desirable propagation performance, many optical fibres have been created and three superior SRHOFs are illustrated in Fig. 2 with regard to nonlinear device application. Here, an inner circle with a radius of $0.8 \mu\text{m}$, which is denoted by a dotted line, contains the core region in each fibre, and randomly small shaded holes represent air regions. And the thickness of each hollow-cylinder-shape layer is equally $1.2 \mu\text{m}$. In terms of nomenclature, the holey optical fibres in Figs. 2(a), 2(b), and 2(c) are named as SRHOF-1, 2, and 3, respectively. The AFs of the designed optical fibres in Fig. 2 are summarized in Table 1.

For example, the SRHOF-1 in Fig. 2(a) is built with the AFs of the first hollow-cylinder layer (AF1), the second (AF2), and the third (AF3) equal to 0.394, 0.205, and 0.181, respectively. As noticed, the SRHOF-2 and 3 both have stepwise-increasing AFs from the core to outer cladding.

Table 1. AF parameter values in each hollow-cylindershape layer for the designed optical fibres

Fibres	AF1	AF2	AF3
SRHOF-1	0.394	0.205	0.181
SRHOF-2	0.304	0.381	0.532
SRHOF-3	0.378	0.403	0.567

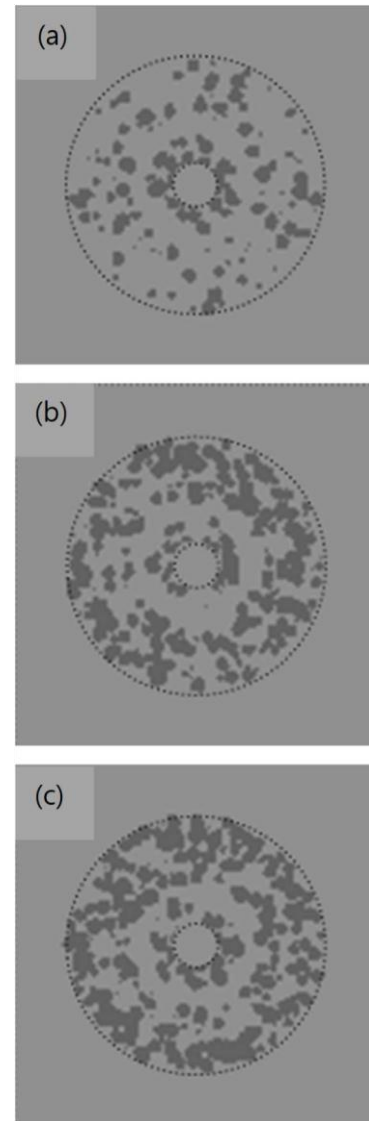


Fig. 2. Three stepwise random-air holey fibres with concentric cladding layers: (a) SRHOF-1, (b) SRHOF-2, and (c) SRHOF-3

III. ANALYSIS AND RESULTS

Along with the design of the stepwise random-air holey fibres, analysis and evaluation have been performed, based on accurate numerical approaches. Two computational techniques are employed in pursuit of several optical transmission properties such as normalized propagation constants, chromatic dispersions, electromagnetic fields, and effective areas. One technique is the finite-difference time-domain (FDTD) method [19–21], which is an effective approach for calculation of propagation constants of guided modes. In this method, the continuous electromagnetic field is sampled at distinct points in a finite volume of space and at equally spaced sampling points in time. The sampled data are then used for numerical calculations of allowed modes in a given waveguide. And the other one is the finite difference method (FDM) [22,23]. By using this algorithm, the computation of field components is more readily accomplished on the basis of the determined propagation constant of a mode.

Using the rigorous full-vectorial FDTD and FDM techniques, which are preferred for the accurate computation of light-guidance characteristics, the feasibility of whether or not the proposed SRHOF can support the single fundamental mode is explored at the beginning of this research. Then, based on the normalized propagation constant results, the chromatic dispersion of the identified mode is computed, considering to allow its value to vary possibly up to a large, negative dispersion parameter for better dispersion tailoring and thereby regain much of original shape from a broadened pulse [14,24]. As for the dispersion computation, the FDM approach is excellently adopted for the examinations of electromagnetic field and effective area as follows.

III.1 Normalized Propagation Constants

Since the proposed random-hole optical fibres guide light desirably in close to the core, several optical properties have been investigated using the two numerical computation techniques. For initial investigation of the wave-guidance properties of the SRHOFs, the FDTD is accessed to the optical fibre shown in Fig. 2(a) and the normalized propagation constant is depicted by the solid curve with the star symbols in

Fig. 3(a). For comparison and verification, the FDM is also utilized to perform the computer-simulation of the SRHOF-1. And almost the same effective refractive index is observed over the operating wavelength (λ) range from 0.8 to 1.7 μm , as indicated by the dashed curve. For the case of the SRHOF-2, the normalized propagation constants from the two methods are plotted in Fig. 3(b) and the results agree very closely.

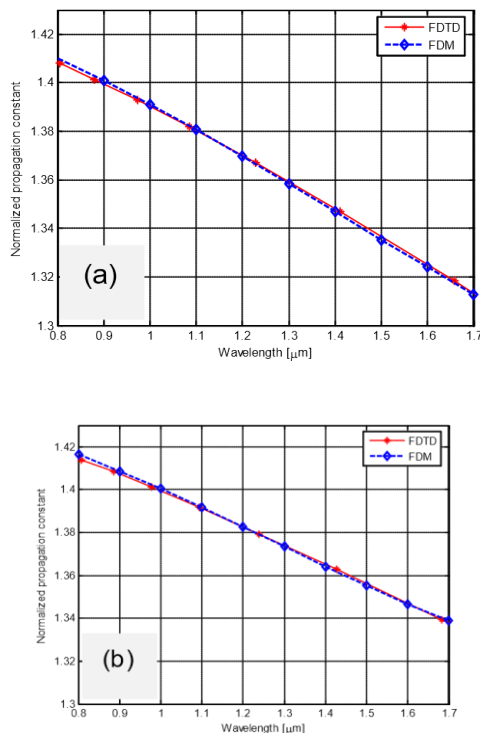


Fig. 3. Comparison of normalized propagation constants from FDTD and FDM analyses for the fundamental mode in each designed holey fibre: (a) SRHOF-1 and (b) SRHOF-2

During this extensive research, it is noticed that the designed random hole fibres guide only the single dominant mode, which is unique characteristic of the typical PCF, over the operation wavelength of interest. Figure 3 also indicates that the SRHOF-1 with the AFs of decreasing step outwards has generally smaller propagation constant, compared to the SRHOF-2 with the stepwise increasing AFs, since the AF1 value close to the core of the SRHOF-1 is larger than that of the SRHOF-2, reasonably.

III.2 Chromatic Dispersions

By differentiating the normalized propagation constant results with the consideration of the material dispersion through Sellmeier's empirical relationship [13], the chromatic dispersion (D_{ch}) is readily computed using the following expression:

$$D_{ch} = \frac{\lambda d^2 \bar{\beta}}{c d \lambda^2} \quad (1)$$

where c is the speed of light in free space and $\bar{\beta}$ represents the normalized propagation constant. Figure 4 shows variations of the dispersion versus wavelength for the SRHOF-2 and 3. It is optimistic result that the chromatic dispersion for the SRHOF3 is about $-186.79 \text{ ps}\cdot\text{nm}^{-1}\cdot\text{km}^{-1}$ at $\lambda = 1.55 \mu\text{m}$, whereas the dispersion for the SRHOF-2 is nearly zero around $\lambda = 1.3 \mu\text{m}$.

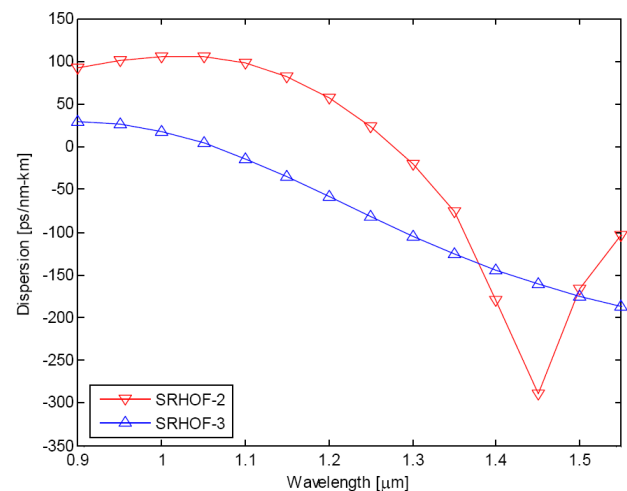


Fig. 4. Chromatic dispersion versus wavelength for the fundamental mode in the designed stepwise random-air holey fibres

Compared with the gradually decreasing dispersion from about zero over the wavelength range from 1.0 to 1.55 μm for the SRHOF-3, the chromatic dispersion for the SRHOF-2 case changes very extensively from 106.06 to about $-289.7 \text{ ps}\cdot\text{nm}^{-1}\cdot\text{km}^{-1}$. It is here mentioned that the FDTD method does not easily accommodate the wavelength dependence of refractive indices, thus the FDM algorithm is preferable for the calculation of field components and suitably employed for the

proposed complicated microstructures with practical design parameters.

III.III Electromagnetic Field Characteristics

In order to appreciate the confinement of electromagnetic fields to the central region, individual mode field distributions are obtained using the FDM, which can quickly and accurately provide individual mode solutions. Figure 5 illustrates the normalized field patterns of the Ex electric component for the dominant fundamental mode at the operating wavelength of 1.55 μm . Figure 5(a) is for the SRHOF-1, while Fig. 5(b) shows the comparison of the Ex field profiles for the SRHOF-1 and 3 on the abscissa micrometer from the core center. As noticed desirably, the power flow density is largest in the central core region of each designed random air-hole fibre.

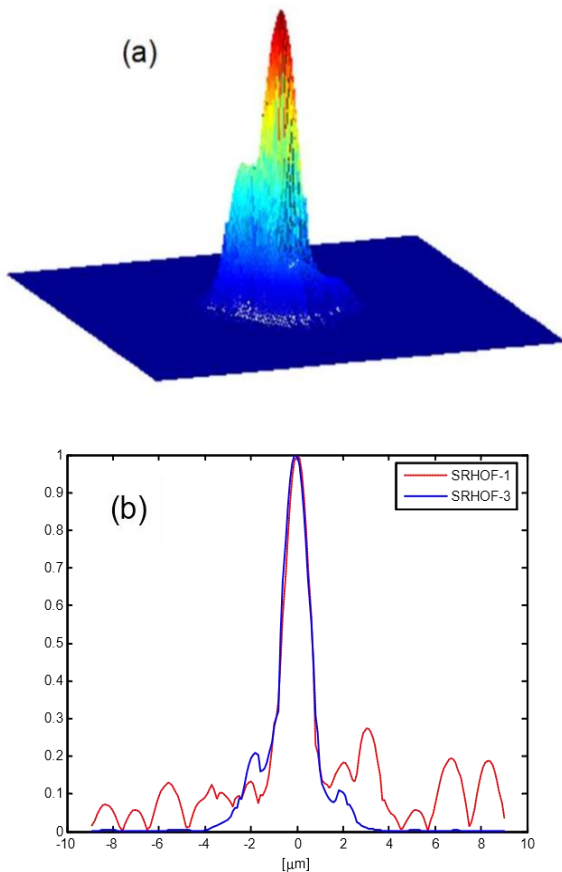


Fig. 5. Normalized Ex field distributions for the fundamental mode at 1.55 μm : (a) 3-dimensional view for the SRHOF-3 and (b) 2-dimensional field profiles for comparison

Although both fibres generate small side-lobes around relatively steep peak, it is observed that the field for the SRHOF-3 is more entirely confined to the core region than that for the SRHOF-1. This is due to the fact that electromagnetic fields tend to have larger concentrations in regions of higher refractive index. This very narrow power concentration is an additive advantage to achieve high nonlinearity.

Once the fundamental mode field results have been obtained, the effective core area that is a key parameter in nonlinear fibre optics can be calculated by using the electric field distribution. The effective areas of the proposed random optical fibres are summarized in Table 2. Since the nonlinearity is inversely proportional to the effective area [25], smaller effective core area is generally preferred in this sense.

Table 2. Effective areas (A_{eff}) for the designed stepwise random-air holey fibres

Holey fibres	A_{eff} [μm^2]	
	$\lambda = 1.3$ [μm]	$\lambda = 1.55$ μm
SRHOF-1	35.909	56.493
SRHOF-2	3.810	8.906
SRHOF-3	3.084	4.942

As noted in Table 2, generally fields spread more into the cladding region at longer wavelengths, resulting in larger values up to $119.567 \times 10^{-12} \text{ m}^2$ at the operating wavelength of 1.55 μm for the effective area. It is also noticed that the effective areas for the SRHOF-1 tend to increase more rapidly with respect to longer wavelengths, compared with those for the SRHOF-2 and 3.

IV. CONCLUSION

Constructing the AFs stepwise-increasing or decreasing outwards from the central core in the cladding region forms new types of optical fibres, SRHOFs, which can desirably support only one strong fundamental mode over the wide operating wavelength range. Based on two computational analyses of the FDTD and FDM for accurate and cross-verified results, it is noticed that the SRHOF with the AFs of increasing step outwards has normally smaller effective core areas at the operating wavelengths of 1.3 and 1.55 μm , compared to the SRHOF with the stepwise-decreasing AFs. By the way, the normalized propagation constant of the former type fibre is generally larger than that of the latter type.

Especially, the SRHOF-3 case fibre provides very small value (about $4.94 \times 10^{-12} \text{ m}^2$) of the effective area, which is highly optimistic for nonlinear devices. In addition, it is also determined that its chromatic dispersion is about $-186.79 \text{ ps}\cdot\text{nm}^{-1}\cdot\text{km}^{-1}$ at 1.55- μm wavelength. Therefore, optical fibre design by adjusting stepwise AFs of random holes in the cladding region should be expected to be beneficial for varieties of dispersion compensation, sensor, and nonlinear fibre applications.

ACKNOWLEDGEMENTS

The author would like to acknowledge the support by the CNU study program (18-0989-01) of Chungnam National University.

REFERENCES

- [1] Joannopoulos JD, Meade RD, Winn JN. Photonic Crystals: Molding the Flow of Light. Princeton University Press. 1995.
- [2] Alexander KA, Akowuah EK, Nukpezah G, Haxha S, Ademgil H. A Theoretical Investigation of a Photonic Crystal Fibre with Ultra-Flattened Chromatic Dispersion with Three Zero Crossing Dispersion Wavelengths. *Optical Fiber Technology*. 2019;53:102032.
- [3] Lavanya A, Geetha G. A Novel Hybrid Hexagonal Photonic Crystal Fibre for Optical Fibre Communication. *Optical Fiber Technology*. 2020;59:102321.
- [4] Birks TA, Knight JC, Russell PSJ. Endlessly SingleMode Photonic Crystal Fiber. *Opt Lett*. 1997;22(13):961–963.
- [5] Kim JI. Investigation of Cladding Effects on Optical Guidance of Microstructured Holey Fibres Based on FDM and FDTD Methods. *Jour Modern Opt*. 2009;56(9):1091–1095.
- [6] Monro TM, Bennett PJ, Broderick NGR, Richardson DJ. Holey Fibers with Random Cladding Distributions. *Opt Lett*. 2000;25(4):206–208.
- [7] Pickrell G, Kominsky D, Stolen R, Ellis F, Kim J, Safaai-Jazi A, et al. Microstructural Analysis of Random Hole Optical Fibers. *IEEE Photonics Tech. Lett*. 2004;16(2):491–493.
- [8] Sharma DK, Tripathi SM. Analysis of the Beam Divergence for One-Rod Core Microstructured Optical Fibres. *Opto-Electronics Review*. 2019;27(2):224–231.
- [9] Liao J, Huang T. Highly Nonlinear Photonic Crystal Fiber with Ultrahigh Birefringence Using a Nano-Scale Slot Core. *Optical Fiber Technology*. 2015;22:107–112.
- [10] Cucinotta A, Selleri S, Vincetti L, Zoboli M. Holey Fiber Analysis through the Finite-Element Method. *IEEE Photonics Tech. Lett*. 2002;14(11):1530–1532.
- [11] Hasan MR, Anower MS, Hasan MI. Polarization Maintaining Highly Nonlinear Photonic Crystal Fiber with Closely Lying Two Zero Dispersion Wavelengths. *Opt Eng*. 2016;55(5):056107.
- [12] Hasan R, Akter S, Rana S, Ali S. Hybrid Porous-Core Microstructure Terahertz Fibre with Ultra-Low Bending Loss and Low Effective Material Loss. *IET Communications*. 2018;12(1):109–113.
- [13] Akowuah EK, Gorman T, Ademgil H, Haxha S, Robinson GK, Oliver JV. Numerical Analysis of a Photonic Crystal Fiber for Biosensing Applications *IEEE Jour Quantum Electron*. 2012;48(11):1403–1410.
- [14] Shen LP, Huang WP, Chen GX, Jian SS. Design and Optimization of Photonic Crystal Fibers for Broad-band Dispersion Compensation. *IEEE Photonics Tech. Lett*. 2003;15(4):540–542.
- [15] Hooper LE, Mosley PJ, Muir AC, Wadsworth WJ, Knight JC. Coherent Supercontinuum Generation in Photonic Crystal Fiber with All-Normal Group Velocity Dispersion. *Opt Express*. 2011;19(6):4902–4907.
- [16] Heidt AM. Pulse Preserving Flat-Top Supercontinuum Generation in All-Normal Dispersion Photonic Crystal Fibers. *Jour Opt Soc Am B*. 2010;27(3):550–559.
- [17] Fu HY, Tam HY, Shao LY, Dong X, Wai PKA, Lu C, et al. Pressure Sensor Realized with Polarization Maintaining Photonic Crystal Fiber-Based Sagnac Interferometer. *Appl Opt*. 2008;47(15):2835–2839.
- [18] Li D, Zhang W, Zhou G. Numerical Analysis of a Side Hole Birefringent Photonic Crystal Fiber with High Pressure Sensitivity. *Opt Eng*. 2016;55(9):097106.
- [19] Taflove A, Hagness SC. Computational Electrodynamics: the Finite-Difference Time-Domain Method. Artech House. 2005.
- [20] Muduli N, Achary JSN, Padhy H. Grade-2 Teflon (AF1601) PCF for Optical Communication Using 2D FDTD Technique: a Simplest Design. *Jour Modern Opt*. 2016;63(7):685–691.
- [21] Sharma M, Konar S. Broadband Supercontinuum Generation in Lead Silicate Photonic Crystal Fibers Employing Optical Pulses of 50 W Peak Power. *Opt Commun*. 2016;380:310–319.
- [22] Guo S, Wu F, Albin S. Loss and Dispersion Analysis of Microstructured Fibers by Finite-Difference Method. *Opt Express*. 2004;12(15):3341–3352.
- [23] Dixit A, Tiwari S, Pandey PC. Evanescent-Field Gas Sensing in Photonic Crystal Fiber Containing Plasma Material by Finite Difference Method. *Sensor Lett*. 2017;15(3):276–281.
- [24] Ouyang G, Xu Y, Yariv A. Theoretical Study on Dispersion Compensation in Air-Core Bragg Fibers. *Opt Express*. 2002;10(17):899–908.
- [25] Agrawal GP. Nonlinear Fiber Optics. Academic Press. 2001.